Journal of Catalysis **191,** 62–74 (2000)
doi:10.1006/jcat.1999.2802, available online at http://www.idealibrary.com on IDEAL®

Oxidative Dehydrogenation of Ethane at Millisecond Contact Times: Effect of H_2 Addition

A. S. Bodke,* D. Henning,* L. D. Schmidt,*,[1] S. S. Bharadwaj,† J. J. Maj,† and J. Siddall†

*Department of Chemical Engineering and Materials Science, University of Minnesota, Minneapolis, Minnesota 55455; and †Dow Chemical Company, Midland, Michigan 56874

Received July 6, 1999; revised December 17, 1999; accepted December 22, 1999

The oxidative dehydrogenation of ethane using Pt/α-Al_2O_3 and various bimetallic catalysts operating at ~1000°C and very short contact times is examined with H_2 addition to the feed. When H_2 is added with a Pt catalyst, the ethylene selectivity rises from 65 to 72% but ethane conversion drops from 70 to 52%. However, using a Pt–Sn/α-Al_2O_3 catalyst, the C_2H_4 selectivity increases from 70 to greater than 85%, while the conversion remains ~70%. The process also produces approximately as much H_2 as is added to the feed. Effects of other metal promoters, sphere bed and fibermat supports, preheat, pressure, nitrogen dilution, and flow rate are examined in an effort to further elucidate the mechanism. Deactivation of the Pt–Sn catalyst is examined, and a simple method of regenerating the activity on-line is demonstrated. Possible mechanisms to explain high selectivities to ethylene are discussed. Although the process can be regarded as a simple two-step reaction sequence with the exothermic oxidation of hydrogen or ethane driving the endothermic dehydrogenation of ethane to ethylene, the exact contributions of heterogeneous or gas-phase reactions and their spatial variations within the catalyst are yet to be determined.

1. INTRODUCTION

Ethylene finds widespread use in the chemical industry in the production of many chemicals (1, 2). Although there has been considerable research in alternative processes for ethylene synthesis (3–9), it is now produced almost exclusively by homogeneous pyrolysis, known as steam cracking.

Steam cracking is known to have several shortcomings (10, 11). It is a highly endothermic process, requires long residence times, produces significant amounts of emissions such as NO_x because of flames in the furnace, and requires periodic shutdowns of the reactor because of coking of the reactor walls. Typically steam cracking of ethane is run at ~850°C with a residence time of 1 s and gives ~85% ethylene selectivity on a C-atom basis at ~60% ethane conversion. Thus far, this performance is better than any alternate process to manufacture ethylene from ethane. Hence, despite the above limitations, steam cracking has been the process of choice for olefin synthesis for many years.

Several years ago we showed that the oxidative dehydrogenation of ethane over a Pt catalyst can achieve ~65% ethylene selectivity at 70% conversion (12). Of the 35% of ethane that does not form ethylene, ~25% oxidizes to form CO and CO_2, ~5% forms CH_4, and ~5% forms higher hydrocarbons such as C_3H_6 and C_3H_8. This process typically runs autothermally at around 1000°C and 5-ms residence time. The overall reaction is exothermic and no carbon buildup was experimentally observed over many days of operation. We also showed that use of Pt–Sn catalysts rather than Pt alone gave a slightly higher selectivity of ~70% (13).

We have recently shown that addition of large amounts of hydrogen to the ethane–oxygen feed mixture gives a large increase in selectivity to ethylene (14). This occurs because O_2 reacts with the H_2 to produce H_2O instead of reacting with C_2H_6 to produce CO and CO_2. H_2O formation is highly exothermic and releases a large amount of heat, facilitating the endothermic dehydrogenation reaction of C_2H_6 to C_2H_4 and H_2. While H_2 addition using a Pt/Al_2O_3 catalyst caused the C_2H_4 selectivity to rise from 65% to slightly above 70%, H_2 addition using a Pt–Sn/Al_2O_3 catalyst caused the C_2H_4 selectivity to rise from 70 to 85% while the C_2H_6 conversion remained at ~70% (14, 15). Since these selectivities and conversions are at least comparable to those obtained by thermal pyrolysis, this partial oxidation process appears to compete successfully with steam cracking for ethylene production.

We have also shown recently that >80% selectivity to ethylene with H_2 addition can be achieved with Pt alone by adding Pt directly to the hot alumina foam from an aqueous solution in a syringe (21), rather than by conventional wet impregnation of a Pt salt. This on-line process deposits Pt only near the front face of the alumina foam, rather than uniformly through the catalyst, and this leads to higher ethylene and less CO_x, although the conversion is lower than on Pt–Sn. These results are summarized in Table 1, which compares ethane conversion, temperatures, and

[1] To whom correspondence should be addressed.

0021-9517/00 $35.00

selectivities to various products for Pt, Pt–Sn, and on-line Pt, both with and without H_2 added.

Short-contact-time, high-temperature reactors are of course not new in the chemical industry in that Pt-gauze catalysts have been used for the production of HCN and nitric oxide by oxidation reactions for many decades (16, 17). However, there are few other industrial reactors operating at a residence time less than 0.1 s.

In this paper we attempt to elucidate the mechanism responsible for this behavior by examining quantitatively the effects of preheat, pressure, residence time, dilution, and different catalyst support materials and geometries. We also examine minor products in detail because these may give information about the mechanism, particularly on the role of homogeneous reaction steps.

2. EXPERIMENTAL

Catalysts were prepared by dripping an aqueous solution of hexachloroplatinic acid and other metal salts onto the support. The support typically consisted of a 92% α-alumina monolith with ~0.5-mm pore diameter or 45 pores per inch (ppi), an 18-mm external diameter, and a 10-mm length. The surface area was ~0.1 m^2/g and no washcoat was used. To examine support effects, we also used alumina spheres and ceramic fibermats as supports.

After the platinum solution was dripped uniformly over the support, it was allowed to dry under atmospheric conditions and the salt was decomposed by heating in a furnace at 100°C for 1 h and 600°C for 2 h. To prepare bimetallic catalysts, the platinum was deposited on the support as described above and then another aqueous metal salt solution was dripped on the Pt-coated monolith and dried overnight. It was then heated in the furnace at 100°C for 1 h and 700°C for 2 h. Changes in loading or in procedures had only a small effect on the performance.

The catalyst was placed between two blank alumina monoliths which act as radiation shields, sealed with alumina cloth, and placed in an 18-mm-diameter quartz reactor. Reaction gases flowing through calibrated electronic mass flow controllers were premixed and passed through the tube at superficial velocities of 0.5 to 5 m/s. The reactor operated autothermally at ~1000°C and the heat from the exothermic reaction was sufficient to maintain this temperature. External heat was required only to ignite the reaction and was provided by a Bunsen burner flame placed directly on the tube. At about 200°C, the catalytic reaction ignited and the temperature rapidly rose up to reaction temperature. Then the burner was removed and the reaction zone was insulated to achieve adiabatic conditions.

Product gases were analyzed using an HP 5890 gas chromatograph with a 0.3-m-long Haysep D packed column and a TCD detector. Nitrogen (30%) was used as a calibration standard since it is an inert in the reaction. We analyzed up to C_4 species, and C, H, and O balances always closed within 5%.

3. RESULTS

3.1. H_2 Addition

Pt and Pt–Sn catalysts were prepared on α-Al_2O_3 supports as described in the above section. For results shown in Fig. 1, the weight loading of Pt was ~1% on both catalysts with a typical initial ratio of Sn to Pt of ~3/1 by weight on the Pt–Sn catalyst. The C_2H_6/O_2 ratio was maintained at 2/1, while the total flow rate was held at 5 SLPM corresponding to a superficial velocity (gases at room temperature) of ~0.4 m/s. The outlet pressure was 1.2 atm and nitrogen dilution was 30%. H_2 was added in appropriate amounts holding other flow rates constant so that the total flow rate increased and nitrogen dilution decreased with H_2 addition.

As shown in Fig. 1, on adding H_2 to the Pt catalyst the ethylene selectivity rose from 65 to 70%, but the ethane conversion dropped from 70 to ~50%. Oxygen was always completely converted (>99%). Using the Pt–Sn catalyst, the ethylene selectivity rose from 70 to >85% and the conversion remained ~70%. CO and CO_2 selectivities decreased with hydrogen addition, and the decrease was larger on Pt–Sn than on Pt. Pt–Sn also produced less CH_4, C_3H_6, C_3H_8, and C_4H_{10}, but produced more C_2H_2 and C_4H_8 than on Pt.

It is evident that Pt–Sn is considerably superior to Pt for the oxidative dehydrogenation of ethane. It gives greater selectivity to C_2H_4 and less selectivity to CO, CO_2, and CH_4, with or without H_2 addition. It also results in a much higher ethane conversion.

Figure 2 compares the moles of hydrogen produced with the moles of hydrogen fed to the reactor per mole of oxygen. While the amount of H_2 produced depends strongly on conditions, with a Pt catalyst more H_2 is produced than is fed up to $H_2/O_2 \sim 2$. On Pt–Sn, more H_2 is produced than is fed up to $H_2/O_2 \sim 1.3$. Hence gas separation and recycle should provide sufficient H_2 at least up to $H_2/O_2 \sim 2$ with Pt and $H_2O_2 \sim 1.3$ with Pt–Sn.

We have reproduced these results using several catalysts. All of them give the same trends as described above. For Pt, the selectivity and conversion increase by ~1–2% on decreasing the Pt loading from 5 to 1%. For Pt–Sn, the selectivity and conversion increase on increasing the Sn/Pt ratio to ~3 but the performance does not improve with further Sn addition beyond this ratio.

3.2. Minor Products

In Table 1 are shown the typical selectivities and ethane conversion obtained with uniformly impregnated Pt (left), Pt–Sn (center), and on-line Pt (21) (right), with the last prepared by deposition from solution directly onto the

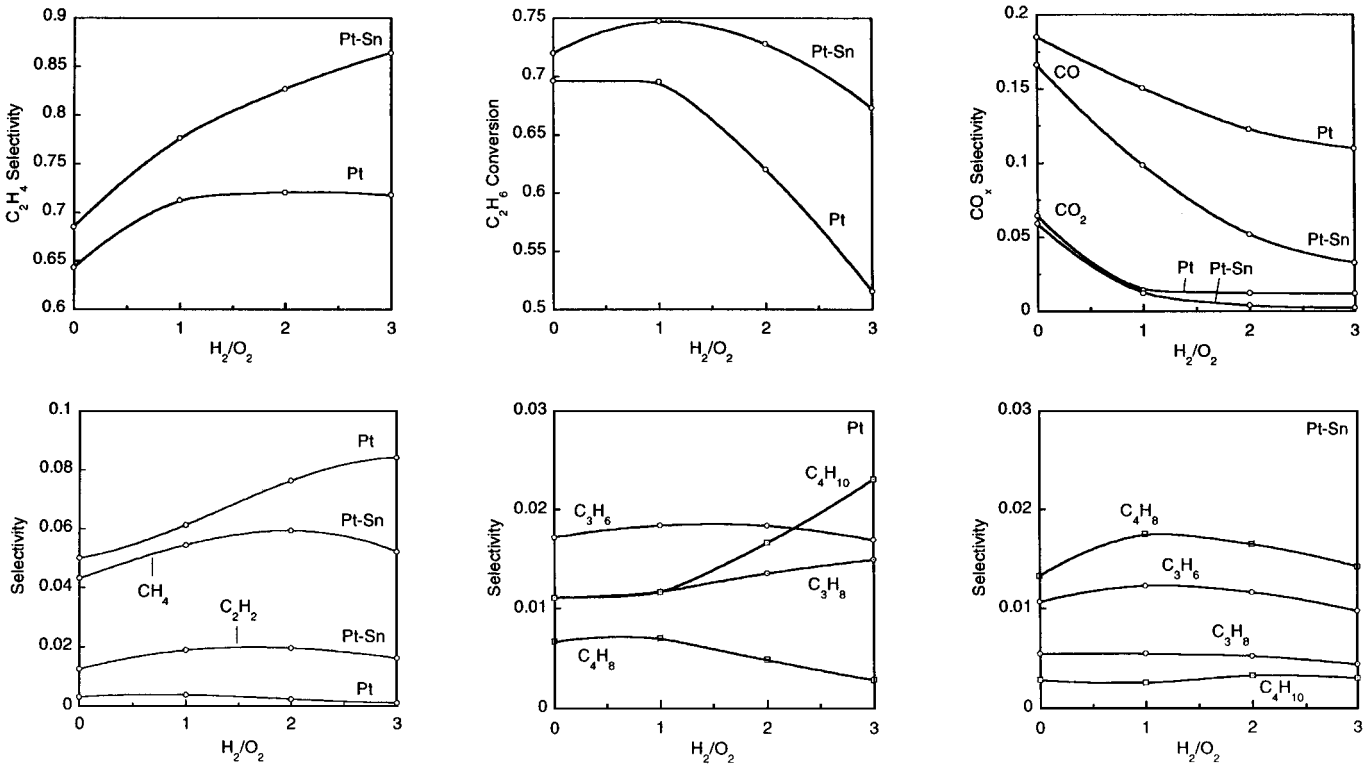

FIG. 1. Comparison of Pt and Pt–Sn catalysts. Selectivity and conversion are plotted as a function of the H_2/O_2 ratio. Pt–Sn produces higher C_2H_4 and lesser CO, CO_2, and CH_4, and gives greater conversion.

hot foam monolith. Shown are typical selectivities with $C_2H_6/O_2/H_2 = 2/1/0$ (no H_2 added) and 2/1/2 (with H_2 added). The on-line Pt catalyst gives a significantly higher ethylene selectivity than uniformly loaded Pt, but the ethane conversion is higher with Pt–Sn than with on-line Pt.

It is seen that CO and CO_2 fall with H_2 addition, while CH_4 remains nearly the same for all catalysts. All other olefins and alkanes up to the C_4 species have less than 2% selectivities, and species above C_4 have less than 1% selectivities.

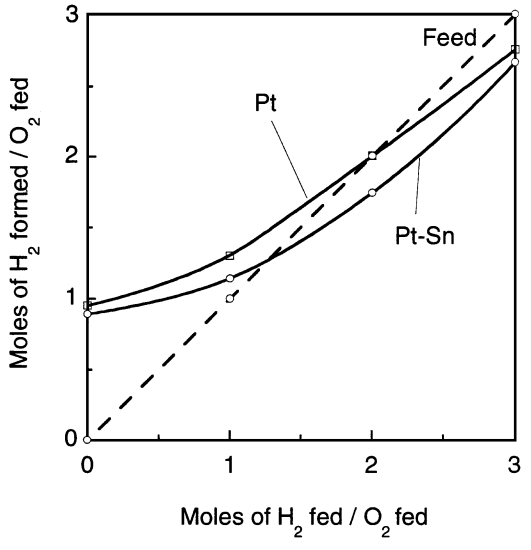

FIG. 2. Comparison of the amount of H_2 fed to that produced using Pt and Pt–Sn. For $H_2/O_2 < 2$ (Pt) and 1.25 (Pt–Sn), the reaction produces more H_2 than that in the feed.

TABLE 1

Experimental Selectivities

	Pt		Pt–Sn		On-line Pt	
$C_2H_6/O_2/H_2$	2/1/0	2/1/2	2/1/0	2/1/2	2/1/0	2/1/2
T (°C)	905	910	943	959	—	—
$X_{C_2H_6}$ (%)	69.6	62.0	72.0	72.8	65.3	63.2
Selectivitiy (%)						
C_2H_4	64.3	72.1	68.5	82.7	65.1	79.2
Total olefins	66.7	74.4	70.9	85.5	66.9	81.3
CO	18.5	12.3	16.6	5.2	21.0	10.0
CO_2	6.5	1.2	5.9	0.4	5.8	0.6
$CO + CO_2$	25.0	13.5	22.5	5.6	26.8	10.6
CH_4	5.0	7.6	4.3	5.9	3.6	5.0
C_2H_2	0.3	0.2	1.3	2.0	0.3	0.4
C_3H_6	1.7	1.8	1.1	1.2	1.2	1.4
C_3H_8	1.1	1.4	0.5	0.5	0.7	0.8
C_4H_8	0.7	0.5	1.3	1.6	0.6	0.7
C_4H_{10}	1.1	1.7	0.3	0.3	1.0	1.3
C_2H_4O	0.7	1.0	0.2	0.2	0.6	0.6
CH_3CHO	0.1	0.2	0.0	0.0	0.1	0.0

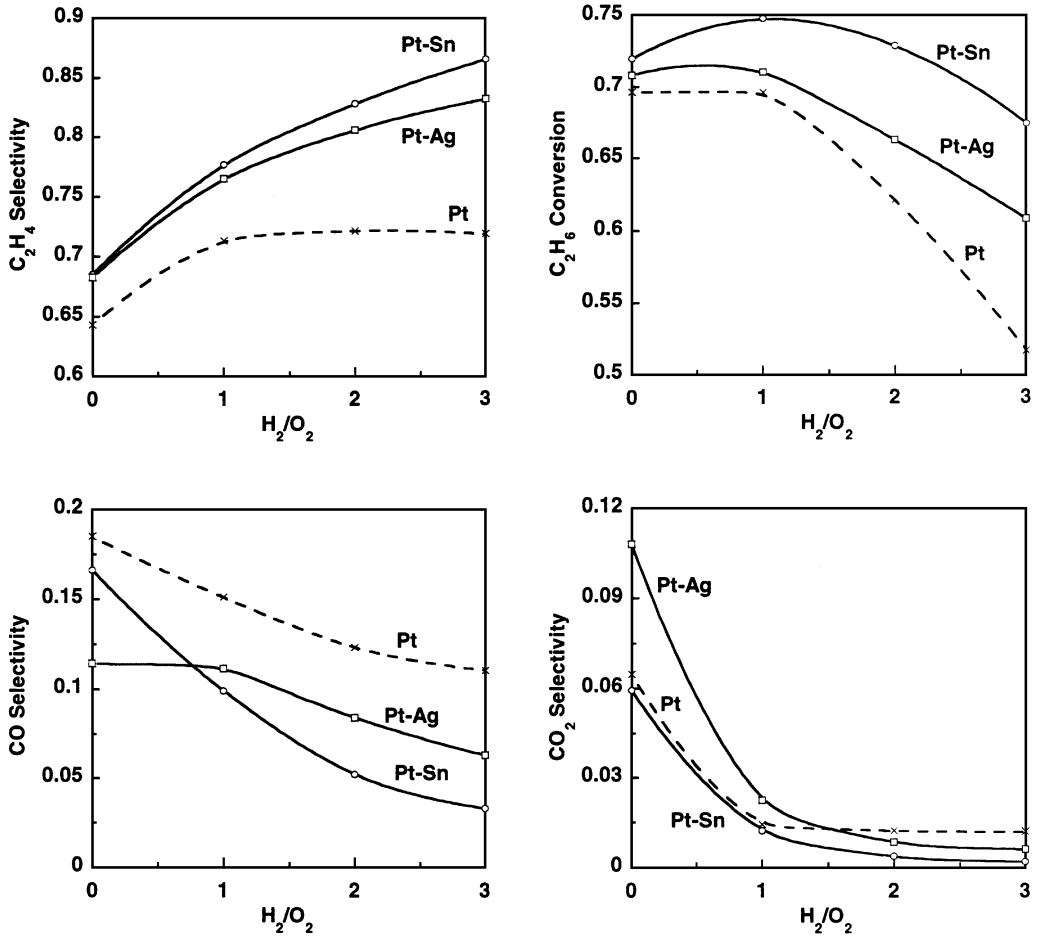

FIG. 3. Effect of addition of Sn and Ag to Pt. Samples were ~2% Pt and 4 wt% Sn and Ag. Both Pt–Sn and Pt–Ag give better ethylene selectivity and ethane conversion than pure Pt catalyst although addition of Ag is not as effective as that of Sn.

The Pt–Sn catalysts give 30% less propylene and 50% less propane than Pt, with or without H_2 added. Butylene is higher with Pt–Sn, while butane is considerably lower. Acetylene goes from 0.2% with Pt to 2% with Pt–Sn.

The dominant oxygenate was ethylene oxide (C_2H_4O), which was much larger than acetaldehyde (CH_3CHO), and all other oxygenates were <0.2% in any experiments. Pt gave much more ethylene oxide than Pt–Sn.

The minor products appear to be formed largely through successive reactions of ethylene: dehydrogenation yielding C_2H_2, dimerization yielding butylene, disproportionation yielding propylene, and epoxidation yielding ethylene oxide.

Any mechanism of this process must account for the observed selectivities of minor products, the differences between catalysts, and the effects of adding H_2.

3.3. Promoters and Supports

We tried various promoters of Pt for this reaction. A detailed investigation of the addition of several metals including Mg, Ce, La, Ni, Co, and Au to Pt has been discussed by Yokoyama *et al.* (13). Figure 3 compares the performance of Pt and Pt–Sn catalysts with of a Pt–Ag catalyst, which gave selectivity and conversion better than those of Pt but lower than those of Pt–Sn. Most of the other promoters studied gave results lower than those of the Pt catalyst.

We also examined various supports with Pt–Sn and H_2 addition. We previously reported minor differences in selectivities and conversions on changing the support material or varying the pore size of the Pt/α-Al_2O_3 monolith from 0.25 to 1 mm (18). Figure 4 compares a Pt–Sn catalyst prepared on a 45-ppi α-Al_2O_3 foam monolith with those using fibermat and sphere-bed supports. The sphere bed was 18 mm in diameter and 10 mm long, and contained nonporous alumina spheres 3.2 mm in diameter. The fibermat was 18 mm in diameter and ~5 mm wide, and contained densely packed, nonwoven alumina fibers 12 μm in diameter.

The C_2H_4, CO, and CO_2 selectivities obtained on all Pt–Sn catalysts were nearly identical. The conversion on the Pt–Sn monolith was slightly higher than those on the fibermat and sphere bed. Support geometry does not appear to

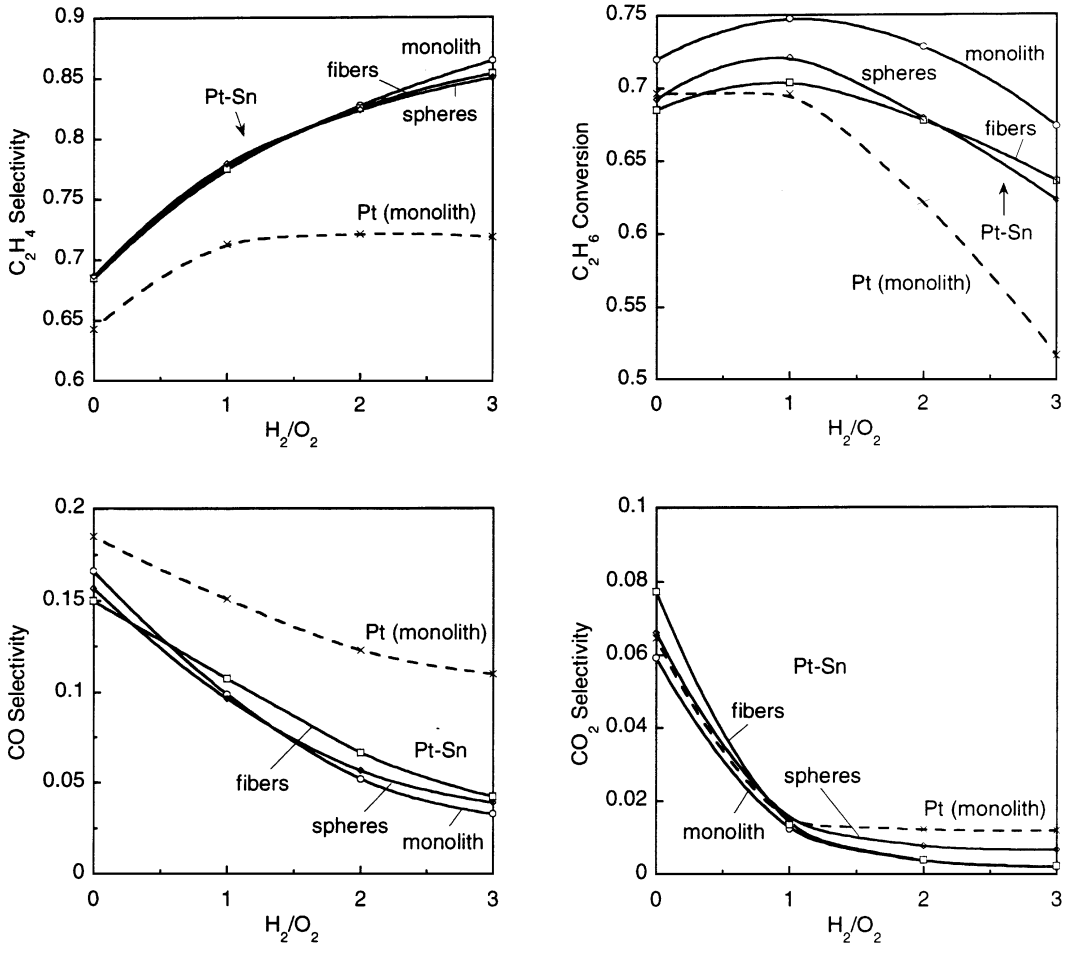

FIG. 4. Comparison of Pt–Sn catalysts prepared on monolith, fibermat, and alumina spheres. Although the support geometry is very different, selectivities and conversion are close on all supports.

play a crucial role in determining catalyst performance as observed previously (18) and in these experiments. The contact time with these supports was ~5 ms, while the reaction goes to completion at contact times as short as 0.5 ms (19). Hickman and Schmidt suggested that the reaction is probably limited by the adsorption of the reactant gases onto the catalyst surface and not by external mass transfer or pore diffusion (20). Hence, the effect of support geometry should not be very significant.

3.4. Stability

While Pt has a melting point of 1775°C, Sn melts at only 230°C. Since the reaction temperature is ~1000°C, one would expect the Pt–Sn catalyst to be unstable under experimental conditions. We investigated the activity of Pt–Sn catalyst with time on stream using 2/1/2 and 2/1/0 ethane/oxygen/hydrogen feeds and both α-alumina monolith and fibermat supports. Figure 5 shows C_2H_4, CO, and CO_2 selectivity and C_2H_6 conversion as a function of the reaction time for the above conditions. Ethylene selectivity and ethane conversion decreased by a few percent over 24 h, while the selectivity to CO and CO_2 increased. As catalysts lost Sn over time, performance of Pt–Sn moved toward that of Pt. However, the deactivation rate was very gradual and the selectivity did not fall below 80% after several hours of operation.

Deactivation seemed to be independent of the input feed composition, and was similar with or without H_2 in the feed. The rate of decrease in the selectivity was much lower than that in the conversion, and the fibermat lost activity faster than the monolith, with or without H_2. However, metal loadings were lower on the fibermat and this may have contributed to the more rapid deactivation.

3.5. On-Line Regeneration

To maximize the production of ethylene, it is crucial to restore activity by replenishing lost Sn in the catalyst. By using an inlet feed system consisting of a rubber septum through which a hypodermic syringe needle is passed and held closely to the front surface of the catalyst, we are able

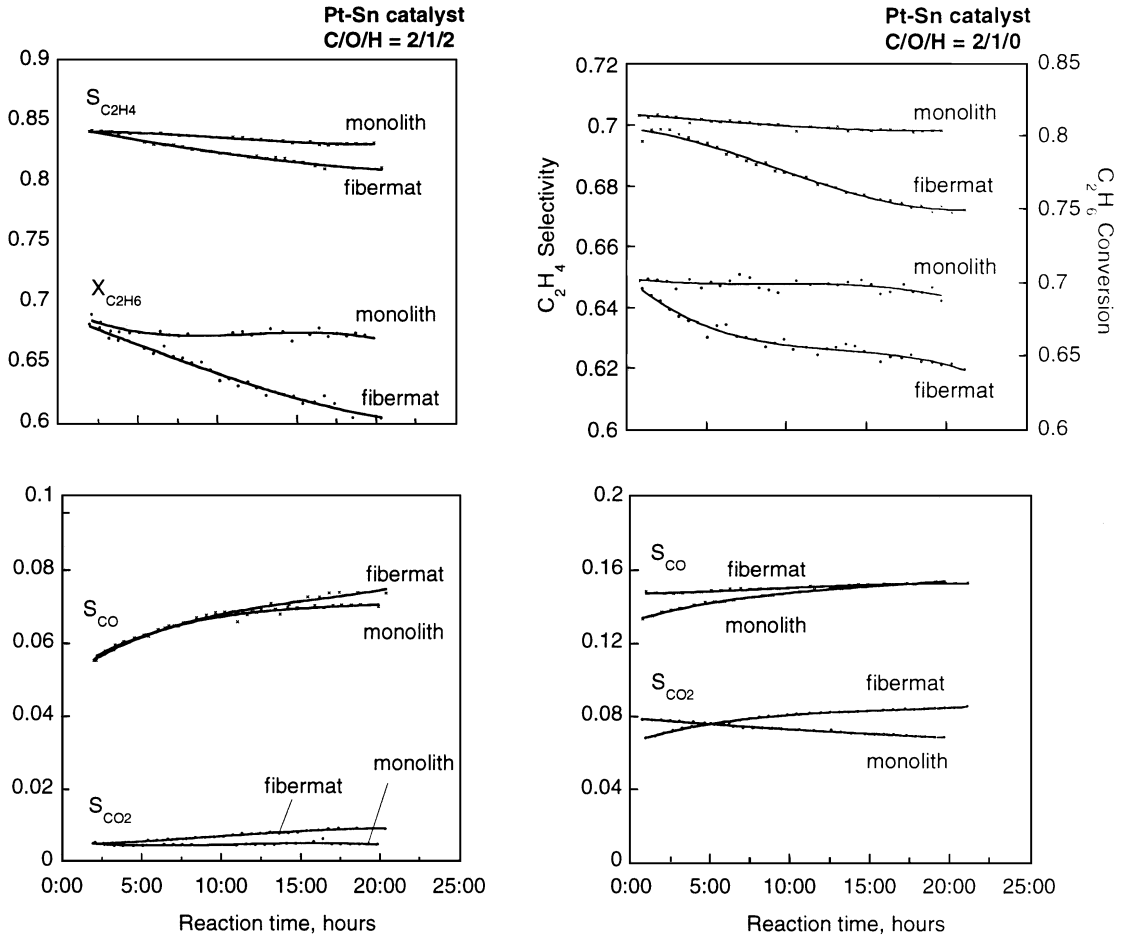

FIG. 5. Time dependence of Pt–Sn catalysts. Selectivity and conversion decrease by a few percent over 24 h on monolith and fibermat supports, with or without H_2. The deactivation rate appears to be higher on the fibermat support.

to add an aqueous solution of $SnCl_2$ to the hot operating catalyst to restore initial performance (21). After ~24 h of operation the C_2H_4 selectivity had dropped from 85 to 83% and C_2H_6 conversion had dropped from 70 to 62% (results in Fig. 5). However, on adding only a few drops of $SnCl_2$ solution, which corresponded to 10 mg Sn on the front surface, the selectivity and conversion increased from 83 and 62% to 84 and 67%, respectively. We reproduced this on-line reactivation experiment multiple times and using different supports.

We conclude that by continuous or intermittent addition of aqueous $SnCl_2$ solution, continuous regeneration of the catalyst should compensate for Sn that is lost from the Pt–Sn catalyst, and the selectivity and conversion can be maintained at the initial values obtained on a fresh Pt–Sn catalyst. This method of regenerating catalysts on-line can also be used to prepare catalysts with active metal deposited only on the front surface of the support in extremely small quantities. Results on such catalysts prepared *in situ* are discussed elsewhere (21).

3.6. Preheat and Pressure

Figure 6 shows the effect of preheat on the performance of a Pt–Sn catalyst. Preheat was applied after the reactant gases were premixed by wrapping a heating tape over the section of the quartz reactor preceding the catalyst. The amount of preheat was varied by changing the current supplied to a Variac connected to the heating tape and the temperatures were recorded using a chromel–alumel thermocouple. On preheating the reactant gases containing a 2/1/2 ethane/oxygen/hydrogen mixture flowing at 5 SLPM and 1.2 atm up to 350°C, C_2H_4 selectivity decreased from 83 to 80%, but conversion increased much more rapidly from 70 to 85%. This led to an increase in the C_2H_4 yield from 58 to 65%. Selectivities to CO, CO_2, CH_4, and C_2H_2 increased on preheating the feed.

The effect of pressure on reactor performance using a 2/1/2 feed mixture flowing at 5 SLPM is shown in Fig. 7. The pressure was varied by adjusting a valve connected in the exhaust line, prior to flaring the product gases in an

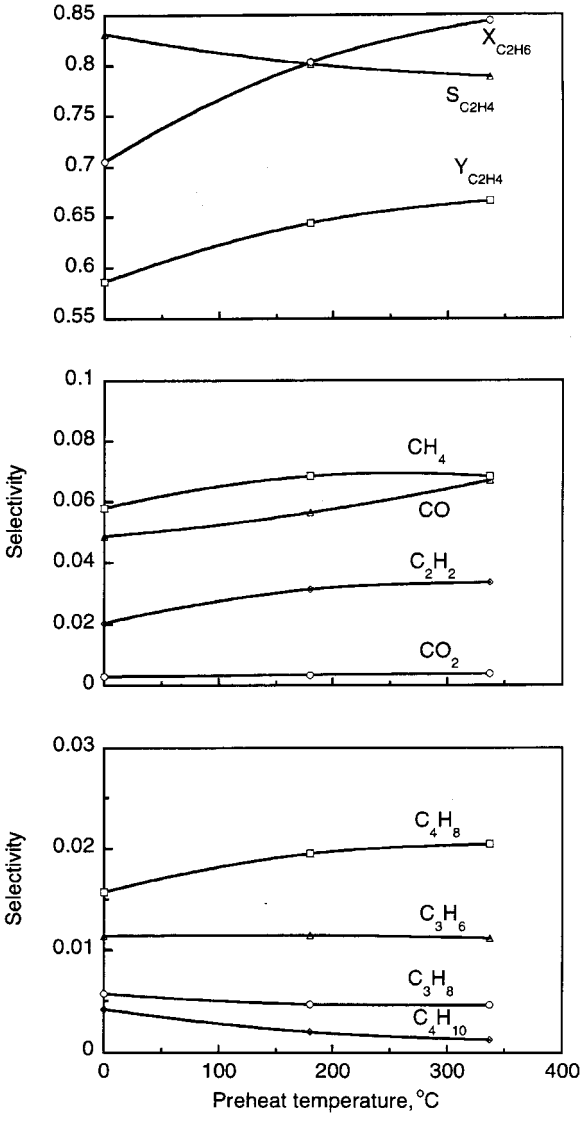

FIG. 6. Effect of preheat on the performance of a Pt–Sn/α-Al_2O_3 catalyst at $C_2H_6/O_2/H_2 = 2/1/2$. The ethylene selectivity decreases and conversion increases with preheat while the ethylene yield increases by more than 7% with 350°C preheat.

incinerator. C_2H_4 selectivity decreased, C_2H_6 conversion increased, and C_2H_4 yield remained nearly constant on increasing the pressure from 1 to ~2 atm. Among the minor products, CO, CO_2, and CH_4 selectivities increased and C_2H_2 selectivity decreased with elevation in pressure.

3.7. Dilution and Flow Rate

Figure 8 shows the effect of nitrogen dilution, under similar experimental conditions. C_2H_4 selectivity increased, but conversion fell rapidly from 75 to 60% on increasing nitrogen dilution from 20 to 50%. CO, CO_2, CH_4, and C_2H_2 selectivities decreased with increasing dilution. The effect of increasing nitrogen dilution seemed qualitatively opposite that of preheating the feed gases as described above.

Changes in selectivities and conversion with flow rate are plotted in Fig. 9. Conditions were otherwise identical to those of earlier experiments. Results seem nearly independent of variation in flow rate from 4 to 16 SLPM. C_2H_4 selectivity and C_2H_6 conversion dropped slightly with increasing flow rate.

3.8. Catalyst Characterization

We have also characterized the surfaces of these Pt and Pt–Sn catalysts using surface analytical techniques such as SEM, XRD, and XPS. Detailed results of these experiments are discussed elsewhere (22). Pt on the α-Al_2O_3 surface is present in the form of spherical, single-crystal, micrometer-sized particles, which are uniformly dispersed throughout

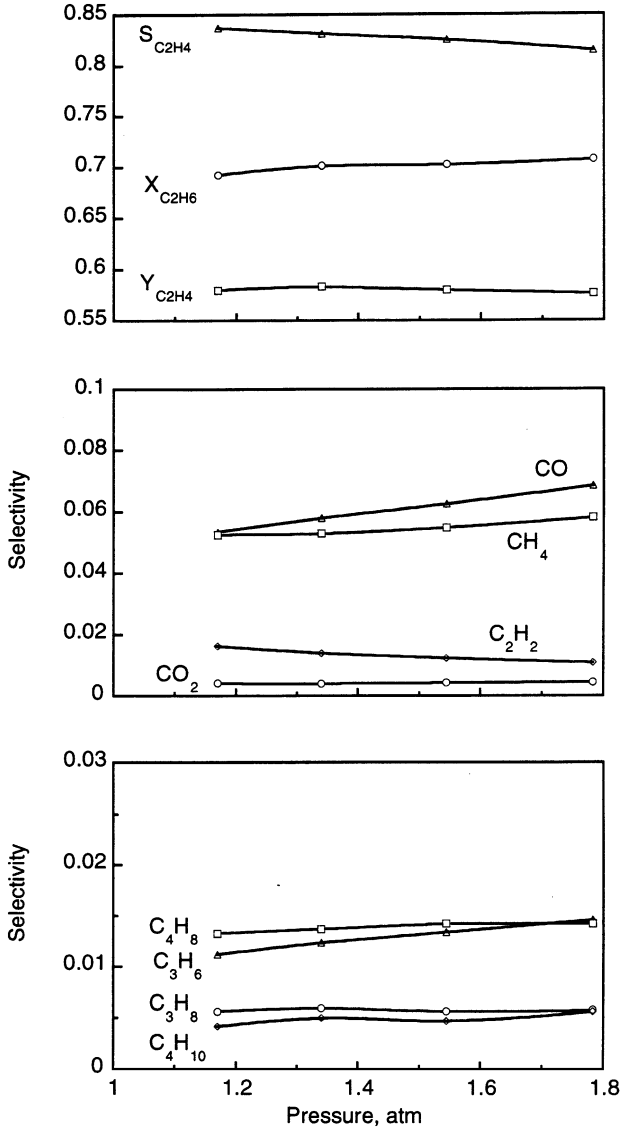

FIG. 7. Effect of pressure on the performance of a Pt–Sn/α-Al_2O_3 catalyst at $C_2H_6/O_2/H_2 = 2/1/2$. The C_2H_4 selectivity drops slightly and the C_2H_6 conversion rises with increasing pressure.

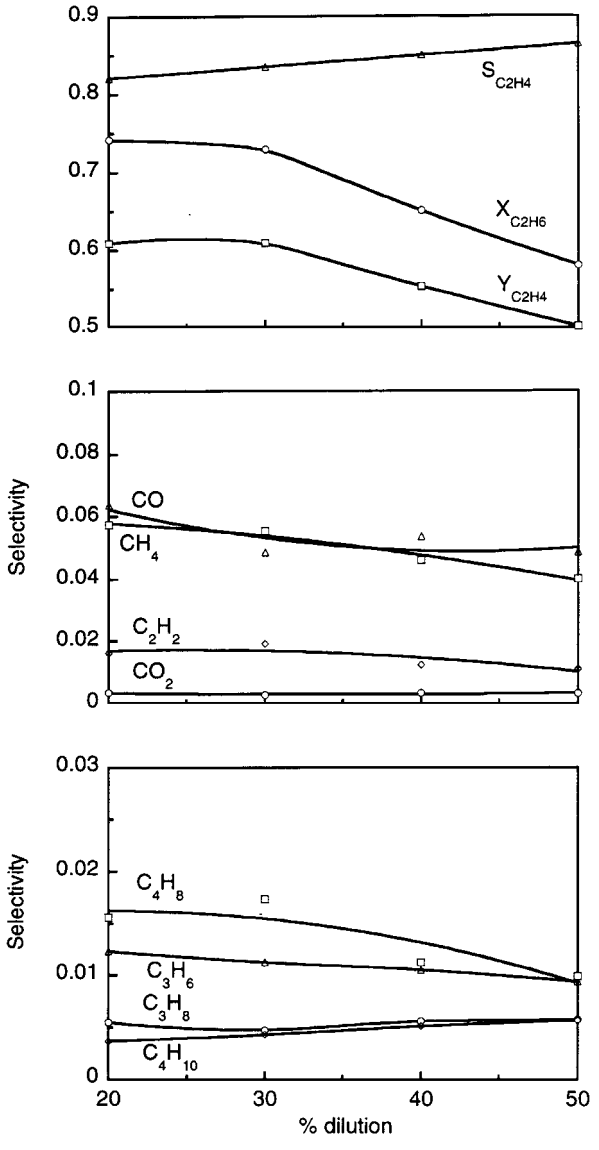

FIG. 8. Effect of nitrogen dilution on the performance of a Pt–Sn/α-Al_2O_3 catalyst at $C_2H_6/O_2/H_2 = 2/1/2$. Ethylene selectivity increases but ethane conversion rapidly falls with increasing dilution.

the support surface. There is no reaction between Pt and the alumina from the support, and the Pt is isolated as multiple fcc crystalline particles. In the case of Pt–Sn, the active catalyst phase is a range of intermetallic compounds, such as Pt_3Sn, PtSn, $PtSn_3$, or a combination thereof. There appears to be no free Pt in that Pt always appears to be associated in compounds with Sn.

4. DISCUSSION

4.1. Mechanism

Hydrogen addition in a 2/1 H_2/O_2 ratio gives a 20% increase in ethylene selectivity with no decrease in conversions for a Pt–Sn catalyst at a 2/1 C_2H_6/O_2 ratio, although for uniformly loaded Pt the corresponding increase is only 5%. We discuss the possible mechanisms for these results in terms of surface versus homogeneous reactions and possible spatial variations in the catalyst.

These experiments show the following:

1. Addition of H_2 with compounds and alloys of Pt strongly suppresses deep oxidation channels while not decreasing ethane conversion.

2. On-line Pt gives selectivities nearly as high as those obtained with Pt–Sn, although conversion is significantly lower. Deposition of Pt only near the front face of the catalyst thus gives performance nearly comparable to that attained with uniform Pt–Sn.

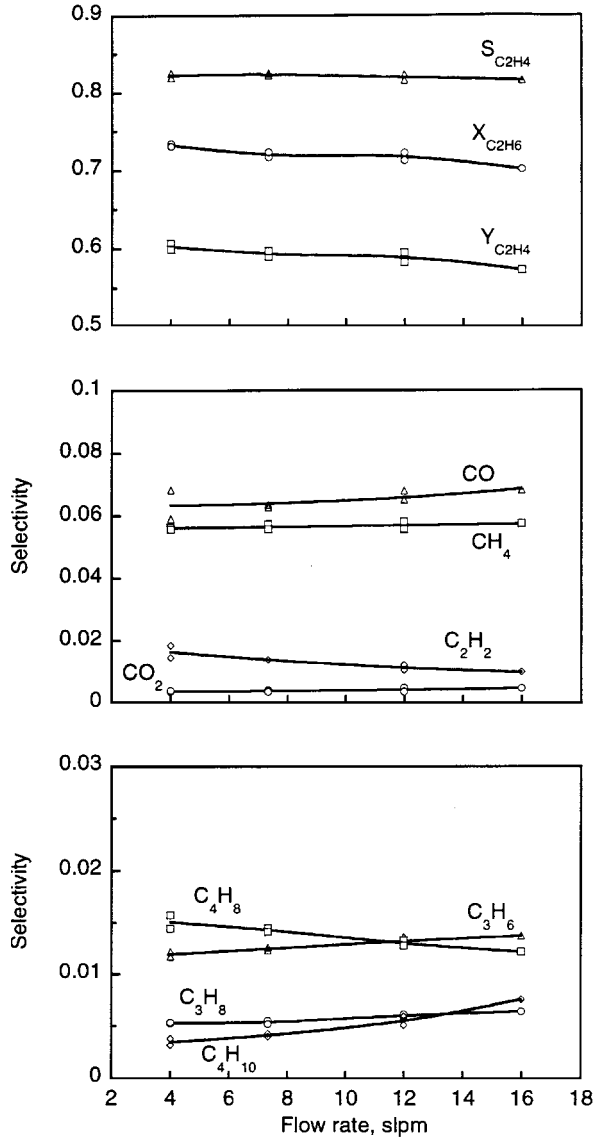

FIG. 9. Effect of flow rate on the performance of a Pt–Sn/α-Al_2O_3 catalyst at $C_2H_6/O_2/H_2 = 2/1/2$. Selectivities and conversion are relatively unchanged with a fourfold change in the flow rate.

3. Conversion and selectivity are nearly independent of flow rate over a large range. Thus the reactions have essentially gone to completion within less than 10^{-3} s, and we have so far been unable to "blow out" the reaction.

4. The performance is largely independent of Pt loading and Pt–Sn ratio over a large variation. This shows that the details of particle size, distribution, and Pt–Sn ratio are not major factors in determining selectivity and conversion.

5. Foams, fibers, and spheres give similar selectivities and conversions gave similar performance. Thus, catalyst support and geometry have a small influence on performance.

6. Preheat, dilution with N_2, and pressure cause only a few percent changes in the process on varying these parameters by factors of $\sim$2.

This process is thus fairly "robust" with respect to variations in most operating parameters except feed composition. Preheat, dilution, and higher pressure changes appear to be explainable through the temperature changes they induce. Thus preheat, absence of dilution, and higher pressures all increase the catalyst temperature which increases ethane conversion while lowering selectivity.

We also note that the processes may be more complex than can be handled quantitatively through the conventional mass and energy balance equations. The temperatures are very high and the gradients are very large, 10^6 K/s and 10^5 K/cm. Most reactions appear to occur within 1 mm of the entrance to the foam where entrance effects cause boundary layers of $<$100-μm thickness. Surface residence times are very short at these temperatures, 10^{-9} and 10^{-12} s for typical adsorbate binding energies of 25 and 5 kcal/mol, respectively. Thus, kinetics measured at low temperatures may not be applicable to these extreme conditions. Also, since reactions proceed nearly to completion within a diameter of the ceramic foam cells, most reactions occur in the entrance region where radial variations in composition area large. For this situation one-dimensional modeling should not be accurate, and two-dimensional simulations should be necessary for quantitative predictions.

4.2. A Two-Zone Model

Qualitatively, we expect concentration profiles versus position in the monolith as sketched in Fig. 10, both without (left) and with (right) H_2 added at $C_2H_6/O_2/H_2 = 2/1/0$ and 2/1/2, respectively. Initially there is a high O_2 partial pressure (gray zone) where oxidation of C_2H_6 and H_2 occurs, leading to CO and CO_2, as well as H_2O. As soon as all O_2 is consumed, only dehydrogenation reactions (and any reaction with H_2O and between other products) can occur. As sketched in Fig. 10, the O_2 zone should be much shorter with H_2 present, leading to much less CO and CO_2.

Note that with H_2 added in the feed, its concentration should first decrease by reaction with O_2 and then increase by C_2H_6 dehydrogenation so that the amounts of H_2 in the feed and in the product are approximately the same (Fig. 2). Detailed calculations with both surface and homogeneous

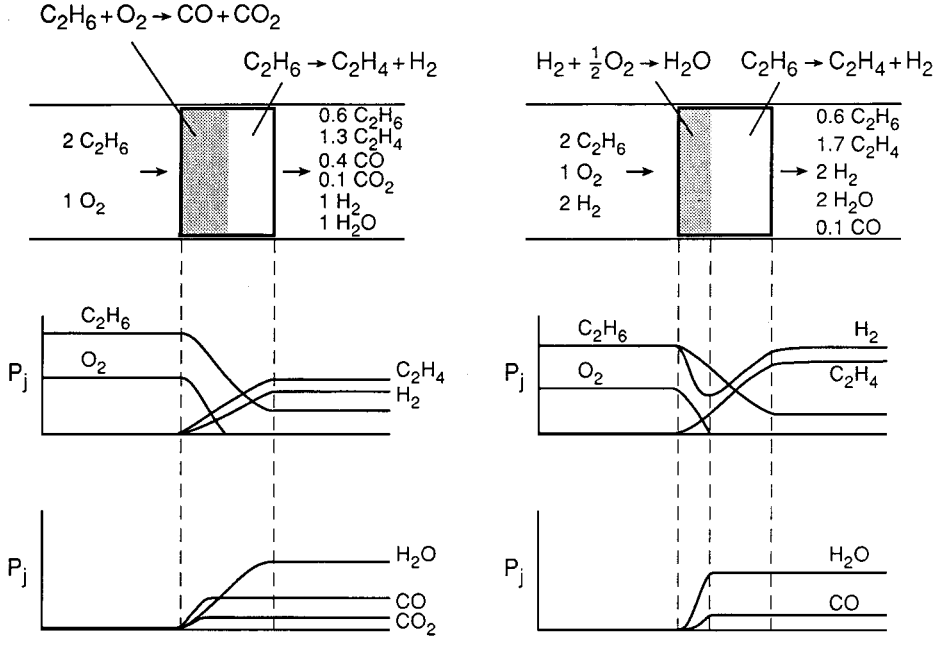

FIG. 10. Feed and exit concentrations and suggested concentration profiles within the monolith without H_2 added (left) and with H_2 (right). The shaded zone indicates the region where oxygen is present. In the absence of H_2, C_2H_6 is partially oxidized to form CO and CO_2, while with H_2 in the feed most O_2 reacts with H_2, leaving C_2H_6 dehydrogenation as the predominant reaction. Note that H_2 initially is converted and then produced such that its feed and exit compositions are approximately equal. The oxidizing shaded zone is probably much shorter than indicated.

reaction steps are required to quantify concentration profiles.

Temperature gradients at the front edge of the catalyst are enormous because the reaction goes to completion at contact times as low as 500 μs which makes it difficult to quantify the mechanism of this process. Furthermore, product compositions are very different than thermodynamic predictions (see below), and, although the feed mixture might be expected to be extremely flammable, no homogeneous flames were visible even for large amounts of hydrogen added to the feed. This suggests that the reactions involving H_2 and O_2 must be occurring primarily on the catalyst surface. However, the contribution of gas-phase chemistry in the dehydrogenation of C_2H_6 to C_2H_4 is not clear. We propose the following mechanism to explain the high selectivities to ethylene obtained in this process.

A Pt–Sn catalyst operating at $C_2H_6/O_2 = 2$ gave ~70% C_2H_4 selectivity and C_2H_6 conversion. Of the 30% C_2H_6 molecules not forming C_2H_4, ~20% formed CO and CO_2, ~5% formed CH_4, and the remaining C_2H_6 formed higher hydrocarbons such as C_3H_6 and C_3H_8. On adding H_2 to the feed, selectivity to CO and CO_2 decreased continuously from 20 to less than 5%. This suggests that with H_2 added the process operates in two distinct steps. In the first step occurring in the front section of the catalyst, C_2H_6 and H_2 react with O_2 to form total oxidation products, CO, CO_2, and H_2O. This exothermic reaction then drives the subsequent endothermic dehydrogenation of C_2H_6 to C_2H_4 in the second zones. As sketched in Fig. 10, these concentration profiles should be very different with and without H_2 added.

Temperatures in regions upstream and downstream of the catalyst were experimentally measured to be constant within at least ~100°C. This, however, does not eliminate the possibility of a steep temperature profile in the upstream section of the catalyst corresponding to highly exothermic oxidation reactions. Such a temperature spike is difficult to determine experimentally, although we observe no large temperature variations in the catalyst. The extent of the dehydrogenation reactions occurring in the downstream section would strongly depend on the temperature profile, and these should take place mostly in the absence of oxygen as shown.

In the early part of the catalyst with significant amount of O_2 in the gas phase, surface characterization experiments coupled with one-dimensional modeling calculations indicate that the surface should be predominantly oxygen covered (52). C_2H_6 and H_2 should dissociatively adsorb on the surface and react with the O radicals to form OH and CO, which can react further to form CO_2. Most of the O_2 is predicted to react rapidly within few molecular layers of the catalyst after which the catalyst surface should become O-deficient. Under these conditions, β elimination of an H atom from adsorbed C_2H_5 radicals should result in formation of C_2H_4 which should rapidly desorb. Alternatively, C_2H_4 could further react to form C_2H_2 and C radicals, eventually forming CH_4 and higher hydrocarbons.

For a 2/1 C_2H_6/O_2 feed using a Pt/α-Al_2O_3 catalyst, experimental results indicate that ~25% of the C_2H_6 reacts in the first section to form CO and CO_2. The remaining C_2H_6 dehydrogenates primarily in the later part of the catalyst to form C_2H_4 and other hydrocarbons such as CH_4, C_2H_2, C_3H_6, and C_3H_8 as listed in Table 1. Addition of H_2 to Pt/α-Al_2O_3 should increase the coverage of surface H atoms, producing more H_2O in the earlier part and more CH_4 in the later part of the reactor. This should increase the C_2H_4 selectivity due to reduction in the formation of CO and CO_2.

Thus Pt–Sn is more selective to the oxidation of H_2 than to that of C_2H_6, compared with Pt alone. Although C_2H_4 selectivities without H_2 addition on both catalysts are not very different, the reduction in CO_x selectivity and the improvement in C_2H_4 selectivity on adding H_2 are considerably greater on the Pt–Sn catalyst than on the Pt catalyst.

4.3. Platinum–Tin Catalysts

Pt–Sn is well known as an excellent hydrocarbon reforming catalyst when supported on alumina, and has shown improved catalytic activity compared with alumina-supported platinum. Catalytic dehydrogenation and reforming of many hydrocarbons have been investigated in great detail (23–30). These experiments were all carried out at lower temperatures in the absence of O_2, but there are also a few examples of Pt–Sn catalysts used for oxidation reactions (31, 32) at lower temperatures.

Much controversy exists in the literature concerning the state of tin, the nature of platinum–tin interactions, and the catalytic effect of Sn on Pt/Al_2O_3 (33) under catalytic reforming conditions. While some studies propose that an alloy is formed (34–36), others suggest that the tin is not reduced to metal but exists as SnO, SnO_2, or a compound containing tin, aluminum, and oxygen (37–40). Li and Koel (41) showed that annealing a Pt–Sn mixture formed Pt–Sn compounds incorporated into the first Pt layer, and that heating to higher temperatures produced a stable alloy structure, which they characterized using LEED techniques. Overbury *et al.* (42) and Paffett *et al.* (43) also showed that Sn added to Pt-covered surfaces was incorporated into the Pt rather than existing as an overlayer. Chojnacki and Schmidt (44) provided experimental evidence that platinum and tin form several intermetallic compounds such as Pt_3Sn, PtSn, and Pt_2Sn_3 in a reducing environment, but that in oxidizing atmospheres, the metals are segregated as Pt and SnO_2 phases. Results of XRD studies described under Results revealed that Pt and Sn exist as intermetallic compounds, such as Pt_3Sn and PtSn in our catalysts. This suggests that the oxidative dehydrogenation reaction occurred in an overall reducing environment, and that the O_2

must be completely converted in the first few molecular layers of the catalyst.

Xu and Koel studied the thermodynamics and kinetics of CO adsorption on Sn/Pt surface alloys and showed that the adsorption kinetics of CO were strongly influenced by the presence of Sn (45). They also demonstrated a strong decrease in the sticking coefficient of CO with increasing concentration of Sn at high temperatures. Peck and Koel studied the influence of Sn on Pt catalysts for the dehydrogenation of cyclohexadiene to benzene (46). They showed that the addition of Sn to Pt(111) surface completely suppressed the decomposition of product benzene without significantly affecting the dehydrogenation of cyclohexadiene.

Some investigators proposed that the effect of Sn on Pt catalysts involves bifunctional and electronic (ligand) effects (31, 47), while Afonso *et al.* suggested that for dehydrogenation reactions the effect of Sn is geometric (48). Coq *et al.* suggested that Sn merely dilutes the Pt surface, effectively reducing the average particle size (49, 50).

These studies agree qualitatively with the results obtained here since Pt–Sn gave higher C_2H_4 selectivity and conversion. Pt–Sn also gave much lesser selectivity to CO, CO_2, and CH_4 than Pt, which is consistent with the claim that presence of Sn reduces rupture of the C–C bond. Larsson *et al.* suggest that Sn increases the ability of Pt catalyst for reaction of hydrogen with surface carbon during dehydrogenation of propane, which is in apparent contradiction to our experimental observations (23).

4.4. Equilibrium Predictions

At temperatures near 1000°C, thermodynamic equilibrium considerations predict that C_2H_4 should react further to form more stable compounds such as C_2H_2, CH_4, CO, and CO_2. Figure 11 shows equilibrium selectivities to C(s) (graphite), CO, CH_4, CO_2, C_2H_2, and C_2H_4 for varying feed compositions calculated at a typical measured reaction temperature of 950°C. Figure 11A (varying C_2H_6/O_2 with no H_2) and Fig. 11B (varying H_2/O_2 at $C_2H_6/O_2 = 2$) show equilibrium selectivities taking into account the formation of graphite in the solid phase together with gas-phase reactions. Figure 11C (varying C_2H_6/O_2 with no H_2) and Fig. 11D

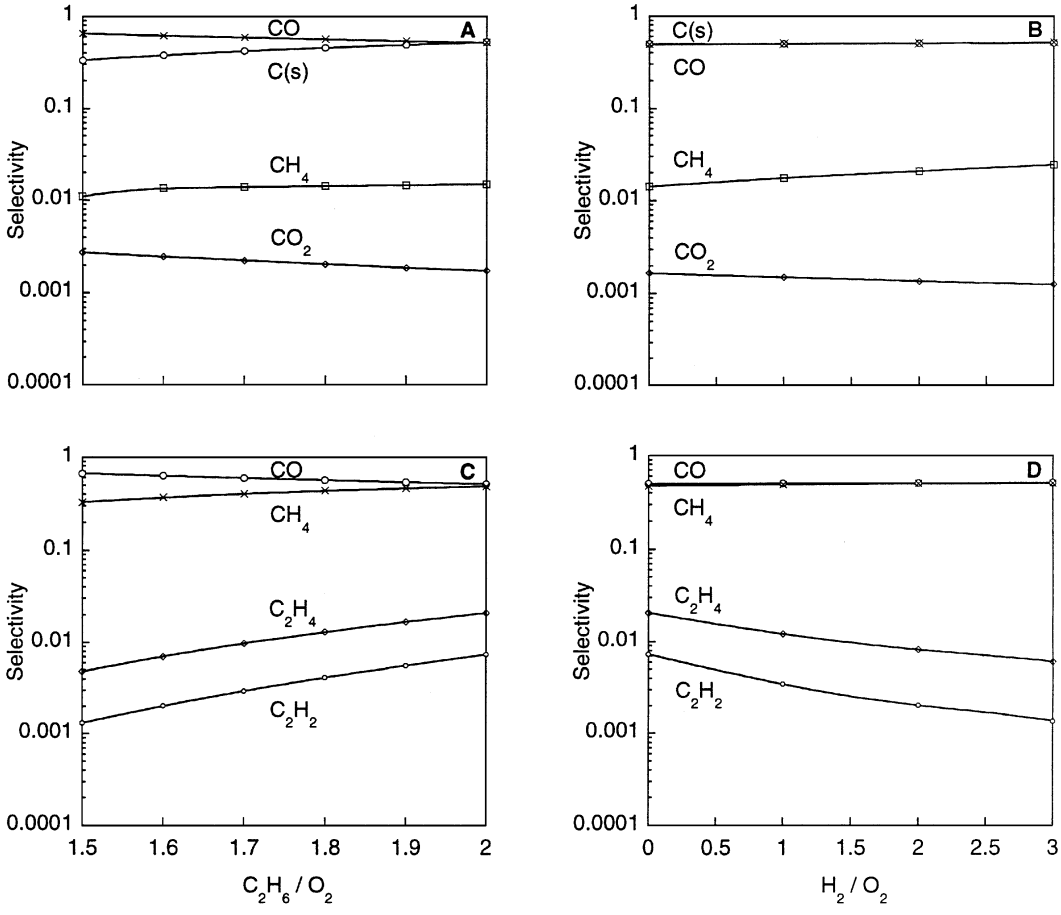

FIG. 11. Equilibrium calculation of product composition for reacting ethane–oxygen–hydrogen mixtures at 950°C (A) and (C) are calculations for selectivities as a function of the ethane/oxygen ratio with no hydrogen added. (B) and (D) show selectivities as a function of hydrogen added for a 2/1 ethane/oxygen mixture. (A) and (B) consider solid carbon formation while (C) and (D) assume only gas-phase reactions.

(varying H_2/O_2 at $C_2H_6/O_2 = 2$) show selectivities assuming only gas-phase reactions with no solid carbon formation.

At equilibrium, solid carbon and CO are the most stable compounds, with or without H_2 addition (Figs. 11A and 11B). CH_4 and CO_2 are also significant with selectivities between 1 and 0.1%. Ethylene, acetylene, and other higher hydrocarbons should be produced at <0.01% selectivity at equilibrium. Assuming no solid graphite formation (Figs. 11C and 11D), CO and CH_4 are the dominant products. In this case, the selectivity to ethylene and acetylene is higher, but is still <1%. The conversion of ethane and oxygen is always complete. These calculations show that ethylene should be highly unstable under experimental conditions with <1% selectivity at equilibrium for all compositions of ethane/oxygen/hydrogen. Graphite, CO, and CH_4 should be the dominant products. Our experimental results are therefore far from equilibrium, indicating that the overall rate of reaction is controlled by kinetic limitations.

4.5. Flames and Explosions

Experiments with ethane/oxygen/hydrogen mixtures may be dangerous because of the highly exothermic and spontaneous reaction of a hydrogen/oxygen mixture. It is known that H_2/O_2 mixtures are flammable (51) in the gas phase over a very wide range of compositions, even with N_2 diluent. However, we observed no homogeneous flames or explosions for any composition of the feed mixture, even at temperatures much above 1000°C. This must be because C_2H_6 not only dilutes the reaction mixture but also quenches radical species that would otherwise lead to chain branching. Homogeneously ethane reacts as rapidly with O_2 as does H_2, so the mixture becomes highly fuel-rich. The endothermic dehydrogenation reaction would also remove heat to further prevent high-temperature excursions.

This reaction system uses the heat produced by an exothermic H_2/O_2 mixture to drive the desired energy-consuming dehydrogenation process. In steam cracking, the heat is released outside the reactor tubes, and heat transfer through these tubes is a slow and rate-limiting process. In oxidative dehydrogenation, the heat is produced and used at reaction sites in close proximity, thus eliminating physical barriers, enhancing heat transfer efficiency, and increasing the overall rate of reaction.

5. SUMMARY

It is possible to produce ~85% selectivity to ethylene at 70% ethane and >99% oxygen conversion using Pt–Sn catalyst and H_2 recycle. These results are at least comparable to those obtained via steam cracking. Furthermore, oxidative dehydrogenation operates at a much shorter residence time, requires no additional heat input, and produces negligible amounts of coke, NO_x, CO_2, and other emissions.

The mechanism clearly involves the initial $H_2 + O_2 \rightarrow H_2O$ catalytic reaction to generate heat and consume all O_2. This is followed by dehydrogenation of $C_2H_6 \rightarrow C_2H_4 + H_2$ which produces as much H_2 as is fed initially. The Pt–Sn surface clearly provides the appropriate surface chemistry to suppress C_2H_6 oxidation to CO and CO_2 while allowing H_2 oxidation to proceed. However, the roles of surface and homogeneous steps are unknown, and a detailed model of this process has not yet been formulated. Full two-dimensional simulations of this process including surface and homogeneous chemistry are in progress.

REFERENCES

1. Weissermel, K., and Arpe, H. J., "Industrial Organic Chemistry." VCH, Weinheim/New York, 1993.
2. "Kirk-Othmer Encyclopedia of Chemical Technology." Wiley, New York, 1991.
3. Le Bars, J., Vedrine, J. C., Auroux, A., Pommier, B., and Pajonk, G. M., *J. Phys. Chem.* **96**, 2217 (1992).
4. Morales, E., and Lunsford, J., *J. Catal.* **118**, 255 (1989).
5. Oyama, S. T., Middlebrook, A. M., and Somorjai, G. A., *J. Phys. Chem.* **94**, 5029 (1990).
6. Skarchenko, V. K., *Int. Chem. Eng.* **9**, 1 (1969).
7. Erdohelyi, A., and Solymosi, F., *J. Catal.* **129**, 497 (1991).
8. Choudhary, V. R., and Mulla, S. A. R., *AIChE J.* **43**, 1545 (1997).
9. Burch, R., C. E. M., *Appl. Catal. A* **97**, 49 (1993).
10. Albright, L. F., Crynes, B. L., and Corcoran, W. H., "Pyrolysis: Theory and Industrial Practice." Academic Press, New York, 1983.
11. Song, Y., Velenyi, L. J., Leff, A. A., Kliewer, W. R., and Metcalfe, J. E., *in* "Novel Production Methods for Ethylene, Light Hydrocarbons and Aromatics" (L. F. Albright, B. L. Crynes, and S. Nowak, Eds.). Marcel Dekker, New York, 1992.
12. Huff, M., and Schmidt, L. D., *J. Phys. Chem.* **97**, 11815 (1993).
13. Yokoyama, C., Bharadwaj, S. S., and Schmidt, L. D., *Catal. Lett.* **38**, 181 (1996).
14. Bodke, A. S., *et al.*, *Science* **285**, 712 (1999).
15. Bodke, A. S., and Schmidt, L. D., U.S. Patent submitted on September 3 (1998).
16. Satterfield, C. N., "Heterogeneous Catalysis in Industrial Practice," 2nd ed. McGraw–Hill, New York, 1991.
17. Pan, B. Y., *Ind. Eng. Chem. Proc. Design Dev.* **8**, 262 (1969).
18. Bodke, A. S., Bharadwaj, S. S., and Schmidt, L. D., *J. Catal.* **179**, 138 (1998).
19. Iordanoglou, D. I., Bodke, A. S., and Schmidt, L. D., submitted for publication.
20. Hickman, D. A., and Schmidt, L. D., *AIChE. J.* **39**, 1164 (1993).
21. Bodke, A. S., and Schmidt, L. D., *Catal. Lett.*, in press.
22. Bodke, A. S., Iordanoglou, D. I., and Schmidt, L. D., in preparation.
23. Larsson, M., Andersson, B., Barias, O. A., and Holmen, A., *Doktorsavhandlingar Chalmers Tekniska Hogskola* **1314**, 233 (1997).
24. Cortright, R. D., Levin, P. E., and Dumesic, J. A., *Ind. Eng. Chem. Res.* **37**, 1717 (1998).
25. Wilde, V. M., Anders, K., and Neubauer, H.-D., *Erdoel Erdgas Kohle* **110**, 463 (1994).
26. Xu, C., Tsai, Y.-L., and Koel, B., *J. Phys. Chem.* **98**, 585 (1994).
27. Durussel, P., Massara, R., and Feschotte, P., *J. Alloys Comp.* **215**, 175 (1994).
28. Aranda, D. A. G., Passos, F. B., Noronha, F. B., and Schmal, M., *Catal. Today* **16**, 397 (1993).
29. Podkletnova, N. M., Kogan, S. B., and Bursian, N. R., *J. Appl. Chem. USSR* **60**, 1872 (1987).

30. Chaouki, J. T., Klvana, A., Bournonville, D., and Belanger, J.-P., *Rev. Inst. Fr. Petrol.* **43**, 873 (1988).
31. Frelink, T., Visscher, W., and van Veen, J. A. R., *Surf. Sci.* **335**, 353 (1995).
32. Anderson, A. B., Grantscharova, E., and Shiller, P., *J. Electrochem. Soc.* **142**, 1880 (1995).
33. Hoflund, G. B., and Asbury, D. A., *Surf. Sci.* **161**, L583 (1985).
34. Lieske, H., *J. Catal.* **90**, 96 (1984).
35. Dautzenberg, F. M., Helle, J. N., Bileon, P., and Sachtler, W. M., *J. Catal.* **63**, 119 (1980).
36. Bacuad, R., Bussiere, P., and Figueras, F., *J. Catal.* **69**, 399 (1981).
37. Muller, A. C., Engelhard, P. A., and Weisang, J. E., *J. Catal.* **56**, 65 (1979).
38. Burch, R., *J. Catal.* **71**, 348 (1981).
39. Burch, R., and Garla, L. C., *J. Catal.* **71**, 360 (1981).
40. Adkins, S. R., and Davis, B. H., *J. Catal.* **89**, 371 (1984).
41. Li, Y., and Koel, B., *Surf. Sci.* **330**, 193 (1995).
42. Overbury, S. H., Mullins, D. R., Paffett, M. T., and Koel, B., *Surf. Sci.* **254**, 45 (1991).
43. Paffett, M. T., Logan, A. D., Simonson, R. J., and Koel, B., *Surf. Sci.* **250**, 123 (1991).
44. Chojnacki, T. P., and Schmidt, L. D., *J. Catal.* **129**, 473 (1991).
45. Xu, C., and Koel, B., *Surf. Sci.* **304**, L505 (1994).
46. Peck, J. W., and Koel, B., *J. Am. Chem. Soc.* **118**, 2708 (1996).
47. Beltramini, J., and Trimm, D. L., *Appl. Catal.* **31**, 113 (1987).
48. Afonso, J. C., Aranda, D. A. G., Schmal, M., and Frety, R., *Fuel Process. Technol.* **50**, 35 (1997).
49. Coq, B., Chaqroune, A., Figueras, F., and Nciri, B., *Appl. Catal.* **82**, 231 (1992).
50. Coq, B., and Figueras, F., *J. Mol. Catal.* **25**, 87 (1984).
51. Lewis, B., and von Elbe, G., "Combustion, Flames and Explosions of Gases," 3rd ed., Academic Press, Orlando, FL, 1987.
52. Huff, M. C., and Schmidt, L. D., *AIChE J.* **42**, 3484 (1996).
53. Ranzi, E., Faravelli, T., Gaffuri, P., D'Anna, A., and Ciajolo, A., *Combust. Flame* **108**, 24 (1997).
54. Mims, C., Mauti, R., Dean, A., and Rose, K., *J. Phys. Chem.* **98**, 13357 (1994).